Advanced Journal of Chemistry-Section A, 2020, *3*, S789–S799 (*Special Issue*)
Available online at : www.ajchem-a.com
ISSN Online: 2645-5676
DOI: 10.33945/SAMI/AJCA.2020.6.9

Original Research Article

Preparation, Characterization and Photocatalytic Application of Novel Bismuth Vanadate/ Hydroxyapatite Composite

Bhawana Khatri, Armila Rajbhandari (Nyachhyon)*

Central Department of Chemistry, Tribhuvan University, Kathmandu, Nepal

ARTICLE INFO

Received: 27 July 2020
Revised: 09 September 2020
Accepted: 21 September 2020
Available online: 24 September 2020

KEYWORDS

Photocatalysis
BHC-composites
MG photodegradation
nanocomposite

ABSTRACT

$BiVO_4$/Hydroxyapatite (HAP) composite was synthesized successfully by combining co-precipitation process and wet-chemical method. Three composites have been prepared by varying the molar concentration of $BiVO_4$ and HAP and were named as 1:1-BHC, 1:2-BHC and 2:1-BHC respectively. These composites were characterized by X-ray Diffraction (XRD), Fourier Transform Infrared Spectroscopy (FTIR), Scanning Electron Microscopy (SEM) and Transmission Electron Microscopy (TEM). SEM and TEM images of as prepared composites revealed the $BiVO_4$ nanorods enclosed with HAP nanoflakes while XRD and FTIR results confirmed the formation of nano composites. The composites were then used as photocatalyst for the photocatalytic degradation of malachite green (MG) dye and the photocatalytic activities were compared with that of $BiVO_4$. The 2:1-BHC showed best MG photodegradation, better than $BiVO_4$ itself due to synergistic effects of adsorption of dye particles by HAP and subsequent photocatalytic degradation by $BiVO_4$. The optimum catalyst dose for 2:1-BHC was found to be 0.1 g per 100 mL of 10 ppm dye concentration with initial pH of solution being 6. These results revealed that BHC-composite did possess the features of visible light active photocatalyst and could be used for the degradation of organic pollutants like dyes.

GRAPHICAL ABSTRACT

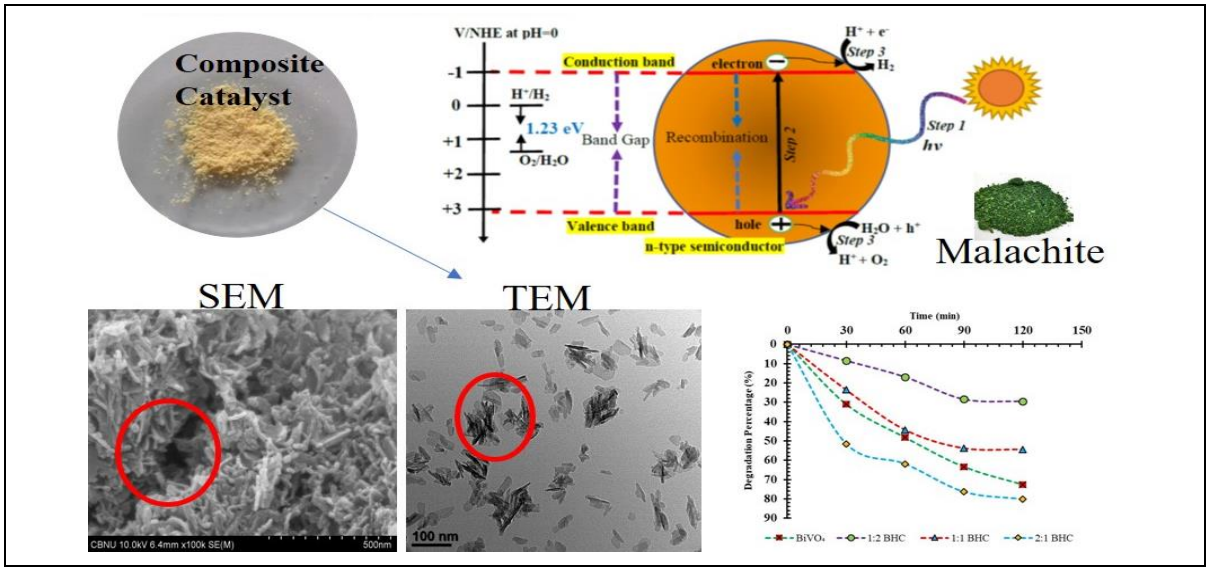

* Corresponding author's E-mail address: armila3@yahoo.com

Introduction

In the recent decade, bismuth-based visible light-active photocatalysts have been extensively used for the removal of pollutants from water. Bi_2O_3 [1,2], $BiVO_4$ [3-7], Bi_2WO_6 [8,9], $BiPO_4$ [1,-11] with narrow band gap (E_g) have been investigated by many research groups. Among them, $BiVO_4$ (E_g=2.4 eV) is one of the widely studied efficient visible light active photocatalyst. It has been used in photocatalytic degradation of organic pollutants in wastewater as well as for photoelectrochemical water splitting resulting hydrogen and O_2 evolution under the sunlight irradiation [12,13].

In our previous work, $BiVO_4$ was used for photocatalytic degradation of the malachite green (MG) dye [14]. In the experiment, there was a problem of dispersion of $BiVO_4$ catalyst in the dye solution and was difficult to separate as well. Similar problems have been stated by other research groups [15]. Additionally, there was a problem of deviation of pH during photocatalytical degradation of MG dye. Therefore, control of pH during the photodegradation experiment is a great challenge. To overcome such problems, many research groups have used dopants or heterojunction with $BiVO_4$ [16]. However, the synthesis of composites with stable support was reported to be one of the most employed methods to improve the material performance. Literatures reported that a stable support can immobilize the active catalyst, increase the surface area of catalytic material, decrease the sintering as well as improve thermal, hydrolytic and chemical stability of the catalytic material [15,17-19]. In the present study, hydroxyapatite (HAP) has been chosen as a supporting material for $BiVO_4$ in form of $BiVO_4$/HAP composites.

The hydroxyapatite (HAP) $Ca_{10}(PO_4)_6(OH)_2$, is one of the common supporting materials that has been used with different semiconductors such as TiO_2 [17,18,20], Ag_3PO_4 [21], $AgBr/Ag_3PO_4$ [21], and BiOCl [22]. HAP was reported to increase the surface area of catalytic material and adsorb pollutant particles for their faster degradation [22]. Yet, it had not been used with $BiVO_4$. In this work, it was used as supporting material with $BiVO_4$ on account of some common features of $BiVO_4$ and HAP such as: both can be synthesized at basic pH [5,21]; both exist in monoclinic forms [3,5,20]; both can be synthesized in nano sizes [5,20]; and both have been used separately in degradation of organic matter with initial solution pH 6 [14, 23]. For synthesis of the composite, facile co-precipitation method for $BiVO_4$ [5] and wet-chemical method for HAP [21,24] have been chosen regarding their simplicity and compatibility.

To study the photocatalytic activity of as prepared $BiVO_4$/HAP composite, malachite green dye (MG) has been used as a model dye pollutant which can undergo photodegradation in presence of a suitable photocatalyst and visible light. Malachite green (MG), a triphenylmethane dye, is a cationic dye with molecular formula $C_{23}H_{25}N_2Cl$ available as chloride salt. It has been used in dyeing paper, leather and silk. It is also utilized as a biological stain; as antibacterial, antiseptic, fungicidal, algicidal and parasiticidal in aquaculture. However, it has been proven to be toxic, irritant, mutagenic and carcinogenic to humans [25-27]. Among various methods of removal of this dye from polluted water, photocatalytic degradation has been proven to be most effective and economic [25]. This process degrades the toxic chemical into smaller eco-friendly products ensuring the complete removal of the dye pollutant [25]. In this study, we report the $BiVO_4$/HAP composites for the photocatalytic activity which is not reported so far and the results were compared with bare $BiVO_4$ to test its efficiency.

Experimental

Reagents

Analytical Reagent (AR) grade bismuth nitrate was purchased from the Merck

Specialties Private Limited, Mumbai and Laboratory Reagent (LR) grade ammonium vanadate (NH_4VO_3) from S.D. Fine Chem. Limited, Mumbai. Calcium nitrate tetrahydrate ($Ca(NO_3)_2.4H_2O$) was obtained from the Rankem (product no. C0480). Di-ammonium hydrogen orthophosphate ($(NH_4)_2HPO_4$) was procured from Thomas Baker Chemicals Pvt. Ltd., India and LR grade 25% ammonia was purchased from Merck life Science private Limited, Mumbai. All the chemicals were used without further purifications.

Instruments

The X-ray diffraction patterns were recorded using Bruker D2 Phaser. A monochromatized Cu Kα (λ= 1.54 Å) radiation working at energy resolution of 180 eV was used. The surface morphology of the as-prepared $BiVO_4$ particles were obtained using mini SEM (Nanoeye, Co.) and those of composites were taken using SU-70, HI-0032-0001 applying current of 120 mA and voltage of 30 kV. Magnified view of the composites was obtained using Transmission electron microscopy (TEM, model Sapera 1 with microscope H7650. The Fourier Transfer Infrared (FTIR) spectra were obtained by using Shimadzu IR Affinity-1 and were recorded from 4000-400 cm^{-1} wavenumber.

Methods

Preparation of $BiVO_4$

$BiVO_4$ was prepared by facile co-precipitation method [5]. Bismuth nitrate solution was prepared by dissolving 1.498 g $Bi(NO_3)_3.5H_2O$ in 100 mL (4M) HNO_3 solution at 70 °C. It was added dropwisely in stirred condition to the ammonium vanadate solution prepared by dissolving 0.362 g NH_4VO_3 in 100 mL (2M) NH_4OH solution. After mixing, the solution pH was adjusted to 9 using (5M) NaOH solution. Then a yellow suspension was obtained. The solvent was evaporated slowly at 70 °C. After complete evaporation, it was calcined at 200 °C. Thus obtained dried material was ground to fine powder. Thus, $BiVO_4$ was prepared.

Preparation of $BiVO_4$/HAP composite

HAP was prepared by wet-chemical method [21]. First of all, the 15 mL of 0.003 mole of $(NH_4)_2HPO_4$ was added dropwisely to the 15 mL of 0.005 mole of $Ca(NO_3)_2$ solution with continuous stirring. A white colored precipitate started to form. After complete addition of $(NH_4)_2HPO_4$, the pH was adjusted to 9 using (2M) NH_4OH solution. Then, a white precipitate of HAP was obtained. As prepared $BiVO_4$ powder was then added slowly in small portions to the HAP containing solution with continuous stirring for 30 min. After addition, stirring was further continued for next 30 min and then left for aging for next 20 h. Then, the solvent was evaporated at 110 °C until all the water got evaporated leaving yellowish white powder. Thus $BiVO_4$/HAP composite was obtained.

Here, $BiVO_4$/HAP composites having three different molar ratios have been prepared. Table 1 shows the molar ratio composition of three different $BiVO_4$/HAP composites which were named as 1:1-BHC, 1:2-BHC, 2:1-BHC.

Table 1. Molar ratio composition of $BiVO_4$/HAP composites

Sample name	Molar Content	
	$BiVO_4$	HAP
2:1 BHC	2	1
1:1 BHC	1	1
1:2 BHC	1	2

Photocatalytic activity

The photocatalytic activities of as-prepared $BiVO_4$ and BHC-composites were measured by degradation of malachite green dye (MG) at ambient temperature. Each degradation study was carried out three times (n=3). A low-cost light simulator was fabricated with a 500 W halogen lamp and was used as the irradiation source. The temperature of the reaction system was maintained at 20-25 °C. For the photocatalytic test, 100 mL of (10 ppm) dye solution was taken in 250 mL beaker. Then, 0.1 g as prepared BHC-composite photocatalyst was added, pH adjusted to 6 [14] and stirred for 15 min for adsorption-desorption process. After that, the solution containing beaker was kept in dark for 30 min for adsorption-desorption equilibrium. Before irradiation, 4 mL of solution was withdrawn for absorbance studies prior to irradiation of light. Then 4 mL of the solutions were pipetted out at every 30 min of irradiation and double centrifugation was done at 4000 rpm for 20 min. Then the absorbance was noted at 617 nm using visible spectrophotometer. Air supply was provided to the reaction system as per needed using air pump from the Silver Lake, model no. SL-2800.

Results and discussion

Phase analysis by X-ray diffraction (XRD)

The XRD patterns of BHCs and pure $BiVO_4$ powders are shown in Figure 1.

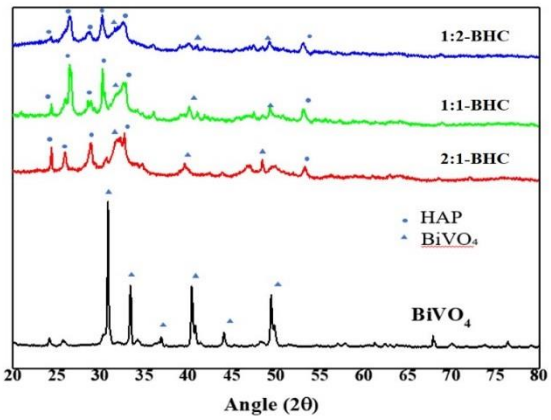

Figure 1. XRD patterns of 1:2-BHC, 1:1-BHC, 2:1-BHC and $BiVO_4$

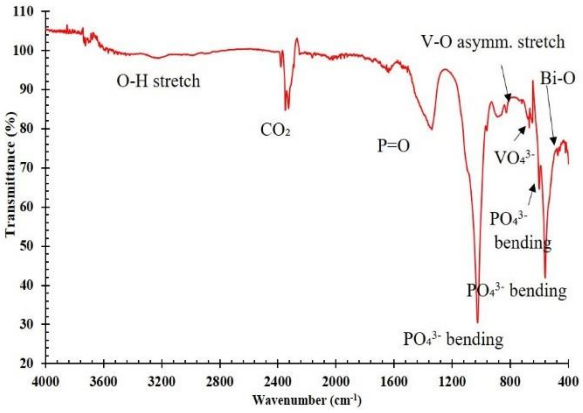

Figure 2. FTIR spectrum of 2:1-BHC

In the XRD patterns of all four prepared catalysts, one can see the major peaks at 30º (121), 33º (040), 40º (211), 49º (116) of 2θ degrees. These peaks are assigned for $BiVO_4$ according to JCPDS card no. 14-0688 [28]. In the BHCs, some new peaks could be observed. These additional peaks at 26º (002), 28º (210), 31.9º (211), 32º (112), 39.5º (310), 47.16º (222), 49.8º (213) of 2θ degrees can be indexed according to JCPDS card no. 09-0423 which corresponds to HAP. These peaks are present along with the peaks of $BiVO_4$ which suggest the coexistence of both $BiVO_4$ and HAP of composite. However, the peaks seem to be broadening with the increase in HAP content and there are some slight shifts in the $BiVO_4$ peaks with the addition of HAP. This may be due to the varying calcination temperature for bare $BiVO_4$ (200 ℃) and BHCs (110 ℃) [29,30]. According to the literature [30], the decreasing calcination temperature leads to broader peaks indicating decreasing crystallinity. Such shifts have been observed in other research works as well [17,31].

Fourier transform infrared spectroscopy (FTIR)

The composite formed between $BiVO_4$ and HAP was further investigated using FTIR analyses to get a better overview of the prepared samples. The FTIR spectrum of 2:1- BHC is shown in Figure 2.

As can be seen from the FTIR spectrum of 2:1-BHC, characteristic bands of phosphate bending at 1024 cm^{-1} and 558 cm^{-1} with a shoulder at 600 cm^{-1} corresponding to PO_4^{3-} are present. Similarly, the band at 1338 cm^{-1} can be assigned to P=O stretch. In additions to these, smaller bands could also be seen at 825 cm^{-1} which corresponds to the asymmetric V-O stretch, at 669 cm^{-1} which relates to VO_4^{3-} and the one at 473 cm^{-1} corresponds to weak Bi-O bond [14]. The bands at around 2327 cm^{-1} and 2349 cm^{-1} correspond to atmospheric/dissolved CO_2. These results are in correspondence with the available literature [31,32]. Hence, the $BiVO_4$ and HAP have been able to form a composite which was clearly observed in the FTIR spectra.

Surface analysis by scanning electron microscopy (SEM)

Surface morphology of the as prepared samples and its particle size were studied using the scanning electron microscopy (SEM). The SEM images of the $BiVO_4$ and BHCs are demonstrated in Figure 3.

Figure 3a shows the SEM image of prepared $BiVO_4$ before calcination at 200 °C. It revealed the rod-shaped structures along with some agglomerated structures. The rod-shaped structures are most probably of $BiVO_4$ and the presence of agglomerated structures probably belongs to the by-products and the non-crystallites. The length of the rods was found to be 1.5 μm and the thickness was found to be 0.5 μm. Such surface morphology was obtained in alkaline pH as per the literatures [4,22].

Figure 3b, c and d illustrates the SEM images of 2:1-BHC, 1:1-BHC and 1:2-BHC respectively. In images b, c and d, brighter rod-like structures were clearly seen which were found to be attached with lighter flake-like structures. The brighter rod-like structures are supposed to be $BiVO_4$ particles which were attached to the lighter HAP flake-like particles [24,33]. The number of dense rod-shaped particles was found to be decreased in SEM images b to d which may be due to decreasing molar ratio of $BiVO_4$. Here, the size of the composite particles was found to be in the nano-size range. The length of the rod-like $BiVO_4$ particles were measured to be 50 nm and width to be 10-20 nm while the size of HAP appears to be varying from 100-150 nm.

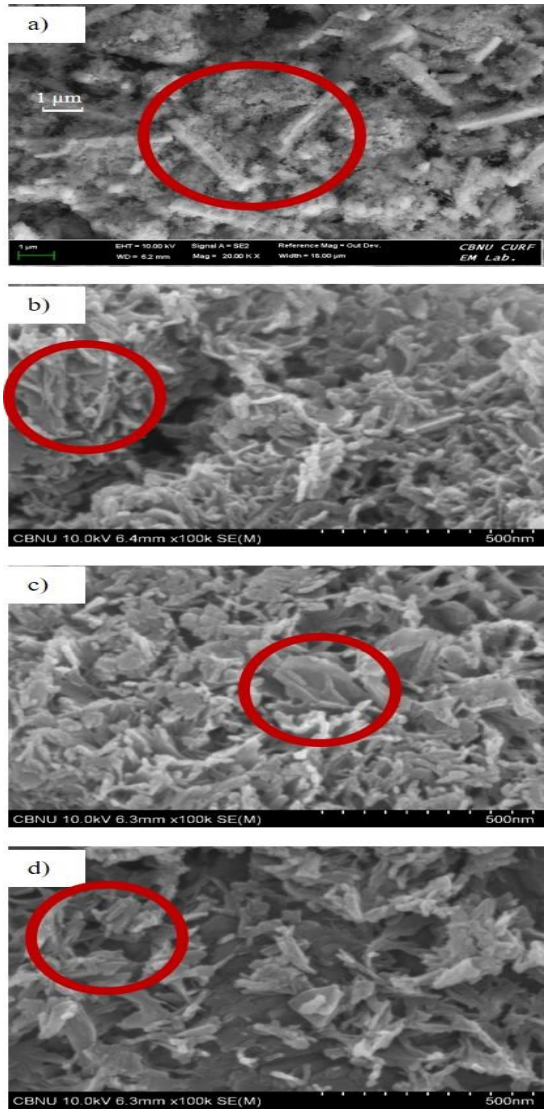

Figure 3. SEM images of as-prepared a) $BiVO_4$ b) 2:1-BHC c) 1:1-BHC d) 1:2-BHC

Transmission electron microscopy (TEM)

The TEM images of all the BHCs are shown in Figure 4 where distinct darker rod-like structures of $BiVO_4$ along with the lighter spread flake-like structures probably of HAP [24] could be clearly seen.

The $BiVO_4$ rod-like particles were found to be scattered in the 2:1-BHC while it was less scattered in 1:1-BHC and 1:2-BHC. In the 1:1 and 1:2 composites, the $BiVO_4$ rods were concentrated in few areas only. Therefore, more homogeneous distribution of $BiVO_4$ is seen in 2:1-BHC.

The distinctly observed denser rods and the lighter flakes leads to a presumption of true formation of composite as the two components are distinct from each other. Since the $BiVO_4$ nanorods are attached to and surrounded by HAP flakes, such attachment can make $BiVO_4$ particles less dispersed in water as HAP is insoluble in water. This result meets the objective of present research work to make the $BiVO_4$ less dispersed in the reaction system.

Photocatalytic degradation studies

In our previous study [14], $BiVO_4$ showed good photocatalytic performance when irradiation was coupled with air supply. Here, the synergistic effect of the lamp light irradiation along with air (O_2) supply led to faster formation of reactive oxygen species ($^{\bullet}OH$, h^+, $^{\bullet}OOH$ or $^{\bullet}O_2^-$) responsible for faster

rate of dye degradation [14]. As described in previous literature, the electron-hole pair (e^--h^+) generated by action of visible light on $BiVO_4$ undergo a series of reactions to generate reactive oxygen species. The reactive oxygen species then react with dye molecules and convert them to harmless products. At this stage, additional oxygen supply from outside accelerates the formation of superoxide anion ($^{\bullet}O_2^-$) which takes part in faster MG degradation. In this study, as prepared BHCs were used in photocatalytic degradation of the MG under lamp light irradiation with air supply. Then, the results were compared with the photocatalytic degradation of MG by $BiVO_4$ in similar physical conditions (Figure 5).

Figure 5 demonstrates the comparison of curves of different photocatalysts at constant initial pH 6, 10 ppm MG solution, same intensity of irradiation and constant supply of air.

As can be seen in Figure 5, four different catalysts showed different rates of photodegradation of MG. The 1:2-BHC and 1:1-BHC showed less photocatalytic activity compared with that of the $BiVO_4$ catalyst while 2:1-BHC displays better activity than $BiVO_4$. In fact, $BiVO_4$ degraded 73.53% of dye while 2:1-BHC degraded 80.20% of dye in 120 min of irradiation. A closer inspection reveals that the 2:1-BHC has degraded significant amount of dye (>50%) within 30 min of irradiation which is higher than any other photocatalysts.

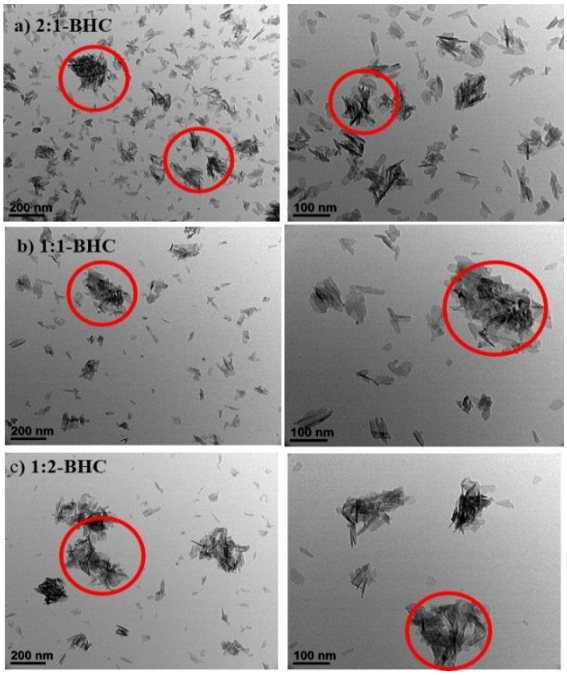

Figure 4. TEM image of a) 2:1-BHC, b) 1:1-BHC and c) 1:2-BHC in 200 nm and 100 nm resolution

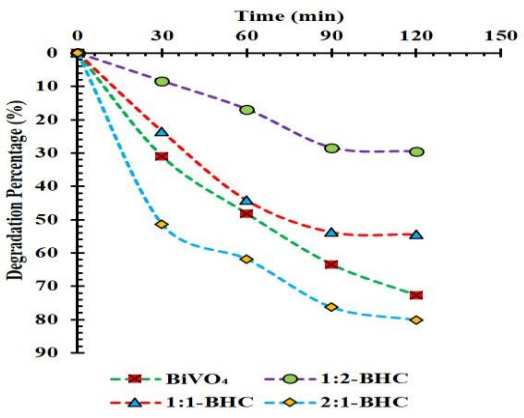

Figure 5. Comparative study of photocatalytic degradation % of MG using $BiVO_4$, 2:1-BHC, 1:1-BHC and 1:2-BHC as a function of time (min)

In this experiment, HAP does not display any significant role as photocatalyst because the band gap of monophasic HAP lies in far UV region (E_g>6 eV) [20]. Hence, the photocatalytic work is exclusively dependent on $BiVO_4$. However, the presence of HAP in BHCs has some effect in the photocatalytic capability of the composites. This might be due to its characteristic adsorbing capability of HAP [34] which adsorbs the dye particles on the catalyst surface and facilitates $BiVO_4$ to degrade dye molecules without itself actually participating in photodegradation of dye. In case of 2:1-BHC, the molar content of both components of the composite appears to be exactly right for the faster degradation of MG dye due to combined effect of adsorption and photocatalytic degradation. However, in case of 1:1-BHC and 1:2-BHC, the decreased molar content of $BiVO_4$ photocatalyst might be the reason for slower degradation of dye.

Here, HAP also revealed the role of supporting material in immobilizing the $BiVO_4$ particles leading to less dispersed $BiVO_4$ particles into the solution.

Similarly, the pH of the solution before and after irradiation was measured (Table 2).

As shown in Table 2, the pH was constant in 2:1-BHC system. So, the spectrophotometric studies are most reproducible in 2:1-BHC composite compared to other prepared composites for the degradation of MG dye.

Therefore, 2:1-BHC demonstrated the best photocatalytic activity in the photodegradation of MG dye. Further studies were then conducted only in 2:1-BHC compared with $BiVO_4$.

Effect of catalyst dose

For this study, the catalyst dose was varied from 0.05 g to 0.2 g with 10 ppm dye concentration, other physical conditions of irradiation, initial pH, air supply and temperature remaining constant.

Table 2. pH of the test solutions before and after irradiation

Photocatalyst	Initial pH	pH after 120 mins
$BiVO_4$	6	7 (± 0.5)
1:2 BHC	6	6.5 (±0.3)
1:1 BHC	6	6.5 (±0.2)
2:1 BHC	6	6 (±0.0)

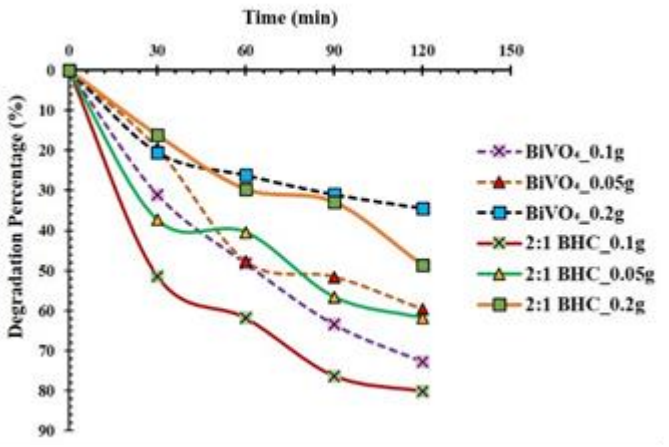

Figure 6. Effect of catalyst dose (g): (a) $BiVO_4$, (b) 2:1-BHC on degradation % of MG

Figure 6 shows the curves of photodegradation rates of MG by $BiVO_4$ and 2:1-BHC as a function of catalyst dose.

As can be seen in Figure 6, both the $BiVO_4$ and 2:1-BHC demonstrated similar characteristics in terms of catalyst dose. The highest photodegradation rate was displayed by 0.1 g photocatalyst dose. Both 0.05 g and 0.2 g catalyst dose exhibited low photocatalytic activity. The decreased degradation rate in 0.05 g may be due to lesser amount of photocatalyst. On the contrary, in the case of 0.2 g catalyst dose, the decreased degradation rate may be due to the turbidity caused by higher dose of catalyst which leads to scattering of light and reducing light penetration to the bottom of the solution [14]. Hence, 0.1 g catalyst per 100 mL dye solution was found to be the optimum catalyst dose for the photodegradation of MG dye. Similar optimum conditions have reported by other literature too [5,31-32].

Effect of dye concentration

Dye concentration of 10 ppm and 15 ppm were tested for their photodegradation by 0.1 g 2:1-BHC catalyst in 100 mL dye solution maintaining similar physical conditions.

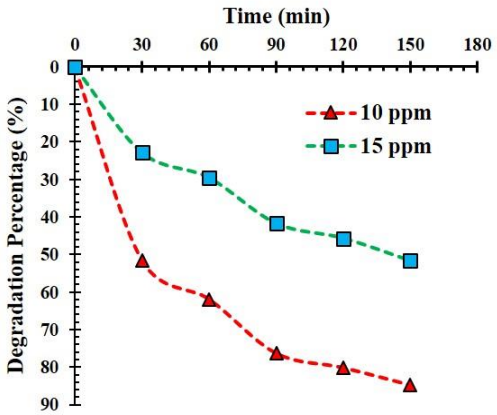

Figure 7. Effect of MG dye concentration (ppm) on photocatalytic action of 2:1 BHC

Table 3. Photodegradation of MG dye for various catalysts

Catalyst used	Irradiation source	Dye concentration (ppm)	Irradiation time (min)	Percentage degradation (%)	Reference
Ir-doped ZnO(5% wt), $K_2S_2O_8$ 0.33 mmol	9W flourescent visible lamp	0.1	120	90	[35]
$Fe_{73.5}Si_{13.5}B_9Cu_1Nb_3$ metallic glass, $K_2S_2O_8$ 1 $mmoll^{-1}$	300W simulated solar lamp	20	30	100	[36]
Naked Nb_2O_5	125W high pressure Hg lamp	5	60	53.25	[37]
$Bi_2O_3/FeVO_4$	500W Xe lamp	20	240	88.7	[38]
$BiVO_4$	500W halogen lamp	10	120	72.73	[14]
2:1 $BiVO_4$/Hydroxyapatite composite	500W halogen lamp	10	120	80.2	This work

As seen in Figure 7, the degradation rate for 10 ppm dye concentration is higher than that of 15 ppm dye concentration. This might be due to the high accumulation of dye particles in the solution which prevents the light to reach onto the catalyst surface. Consequently, the photocatalytical action could not be performed effectively for the degradation of dye.

Comparison with other works

The photocatalytic performance of 2:1-BHC on the photocatalytic degradation of MG dye can be compared with other reported works, as seen in Table 3.

Table 3 suggests that the results of the present work are comparable with previous other reports.

Conclusion

Nanoparticles $BiVO_4$ along with three $BiVO_4$/hydroxyapatite composites (BHCs) were successfully synthesized by co-precipitation method and wet-chemical method, respectively. The XRD, FTIR, SEM, and TEM analyses revealed proper formation of the nanocomposites. The photocatalytic activity of all four photocatalysts was studied for the MG dye photodegradation under 500W halogen lamp irradiation. The 2:1-BHC, consisted of two parts of the $BiVO_4$ and one part of HAP, showed best photocatalytic activity in degradation of MG dye. However, $BiVO_4$ showed better photocatalysis than 1:1-BHC and 1:2-BHC. The enhanced photocatalytic activity of 2:1-BHC might be due to combined activity of the $BiVO_4$ and HAP. Here, $BiVO_4$ acts as active photocatalyst which uses visible light for dye degradation. Supporting it is the HAP, which prevents the dispersion of $BiVO_4$ into the solution owing to the formation of composite. Moreover, HAP also facilitates $BiVO_4$ in faster degradation of dye by rapid adsorption of the dye molecules on the surface of the composite photocatalyst. Therefore, the 2:1 BHC composite exhibited better photocatalytic results. Hence it might be better photocatalyst for the degradation of dyes under visible light.

This study could provide a facile and economic approach to treat the organic pollutants using composites, photocatalysis, and adsorption.

Acknowledgement

This research was financially supported by the University Grants Commission, Nepal under the UGC Masters Research Support, 2018. The Chonbuk National University, Jeonju, South Korea, is acknowledged for providing the SEM images of the $BiVO_4$. Global Research Lab (GRL), Sun Moon University (SMU), South Korea highly acknowledged for providing SEM, TEM and XRD analysis of the composites.

Disclosure statement

No potential conflict of interest was reported by the authors.

References

[1] D. Luo, Y. Kang, *J. Mater. Sci.*, **2019**, *54*, 1549–1565.

[2] Y. Huang, W. Fan, B. Long, H. Li, F. Zhao, Z. Liu, Y. Tong, H. Ji, *Appl. Catal. B Environ.*, **2016**, *185*, 68–76.

[3] Y. Guo, X. Yang, F. Ma, K. Li, L. Xu, X. Yuan, Y. Guo, *Appl. Surface Sci.*, **2010**, *256*, 2215–2222.

[4] G. Xi, J. Ye, *Chem. Commun.*, **2010**, *46*, 1893–1895.

[5] A. Martínez-de la Cruz, U.M.G. Pérez, *Mater. Res. Bull.*, **2010**, *45*, 135–141.

[6] T. Saison, N. Chemin, C. Chanéac, O. Durupthy, L. Mariey, F. Maugé, V. Brezová, J.P. Jolivet, *J. Phys. Chem. C*, **2015**, *119*, 12967–12977.

[7] P. Intaphong, A. Phuruangrat, P. Pookmanee, *Integr. Ferroelectr.*, **2016**, *175*, 51–58.

[8] R. Adhikari, H.M. Trital, A. Rajbhandari, J. Won, S.W. Lee, *J. Nanosci. Nanotechnol.*, **2015**, *15*, 7249–7253.
[9] Y. Zhu, Y. Wang, Q. Ling, Y. Zhu, *Appl. Catal. B Environ.*, **2017**, *200*, 222–229.
[10] J. Cao, B. Xu, H. Lin, S. Chen, *Chem. Eng. J.*, **2013**, *228*, 482–488.
[11] Y. Zhang, S.J. Park, *J. Catal.*, **2017**, *355*, 1–10.
[12] K. Pingmuang, J. Chen, W. Kangwansupamonkon, G.G. Wallace, S. Phanichphant, A. Nattestad, *Sci. Rep.*, **2017**, *7*, 1–11.
[13] P. Luan, J. Zhang, *ChemElectroChem*, **2019**, *6*, 3227–3243.
[14] B. Khatri, I.B. Bamma, A. Rajbhandari, *Int. J. Chem. Stud.*, **2019**, *7*, 595–603.
[15] Y.X. Sun, J. Zhang, *Adv. Mater. Res.*, **2013**, *821–822*, 471–475.
[16] R. Marschall, *Adv. Funct. Mater.*, **2014**, *24*, 2421–2440.
[17] H.R. Han, X. Qian, Y. Yuan, M. Zhou, Y.L. Chen, *Water Air Soil Pollut.*, **2016**, *227*, 461.
[18] S. Murgolo, I.S. Moreira, C. Piccirillo, P.M.L. Castro, G. Ventrella, C. Cocozza, G. Mascolo, *Materials*, **2018**, *11*, 1779.
[19] A. Ibhadon, P. Fitzpatrick, *Catalysts*, **2013**, *3*, 189–218.
[20] C. Piccirillo, P.M.L. Castro, *J. Environ. Manage.*, **2017**, *193*, 79–91.
[21] C. Jia, X. Xie, M. Ge, Y. Zhao, H. Zhang, Z. Li, G. Cui, *Mater. Sci. Semicond. Process.*, **2015**, *36*, 71–77.
[22] P. Raizda, S. Gautam, B. Priya, P. Singh, *Adv. Mater. Lett.*, **2016**, *7*, 312-318.
[23] V. Rajalingam, *Synthesis and Characterization of $BiVO_4$ nanostructured materials: application to photocatalysis*, PhD diss, Université du Maine, **2014**.
[24] V. Rodríguez-Lugo, T.V.K. Karthik, D. Mendoza-Anaya, E. Rubio-Rosas, L.S. Villaseñor Cerón, M.I. Reyes-Valderrama, E. Salinas-Rodríguez, *R. Soc. Open Sci.*, **2018**, *5*, 180962.
[25] L. Yong, G. Zhanqi, J. Yuefei, H. Xiaobin, S. Cheng, Y. Shaogui, *J. Hazard. Mater.*, **2015**, *285*, 127–136.
[26] L.A. Perez-estrada, A. Aguera, M.D. Hernando, S. Malato, A.R. Fernandez-Alba, *Chemosphere*, **2008**, *70*, 2068–2075.
[27] S. Srivastava, R. Sinha, D. Roy, *Aquat. Toxicol.*, **2004**, *66*, 319–329.
[28] H. Jiang, H. Dai, X. Meng, L. Zhang, J. Deng, Y. Liu, C.T. Au, *J. Environ. Sci.*, **2012**, *24*, 449–457.
[29] S.S. Hosseinpour-Mashkani, A. Sobhani-Nasab, *J. Mater. Sci. Mater. Electron.*, **2017**, *28*, 16459–16466.
[30] D.R. Paul, R. Sharma, S.P. Nehra, A. Sharma, *RSC Adv.*, **2019**, *9*, 15381–15391.
[31] H. Yang, S. Masse, M. Rouelle, E. Aubry, Y. Li, C. Roux, Y. Journaux, L. Li, T. Coradin, *Int. J. Environ. Sci. Technol.*, **2014**, *12*, 1173–1182.
[32] L. Berzina-Cimdina, N. Borodajenko, *Infrared Spectrosc. Mater. Sci. Eng. Technol.*, **2012**, 123–149.
[33] N.A.S. Mohd Pu'ad, P. Koshy, H.Z. Abdullah, M.I. Idris, T.C. Lee, *Heliyon*, **2019**, *5*, e01588.
[34] H. Bouyarmane, S. El Asri, A. Rami, C. Roux, M.A. Mahly, A. Saoiabi, T. Coradin, A. Laghzizil, *J. Hazard. Mater.*, **2010**, *181*, 736–741.
[35] N. Babajani, S. Jamshidi, *J. Alloys Compd.*, **2019**, *782*, 533–544.
[36] S.X. Liang, Z. Jia, W.C. Zhang, W.M. Wang, L.C. Zhang, *Mater. Des.*, **2017**, *119*, 244–253.
[37] A.S. Hussein, N.Y. Fairooz, *J. Babylon Univ. Pure Appl. Sci.*, **2016**, 2510–2518.
[38] X. Liu, Y. Kang, *Mater. Lett.*, **2016**, *164*, 229–231.

How to cite this manuscript: Bhawana Khatri, Armila Rajbhandari. Preparation, Characterization and Photocatalytic Application of Novel Bismuth Vanadate/ Hydroxyapatite Composite*, Adv. J. Chem. A*, **2020**, *3*, S789–S799.